This is an open access article published under an ACS AuthorChoice License, which permits copying and redistribution of the article or any adaptations for non-commercial purposes.

ACS OMEGA

Article

Cite This: ACS Omega 2019, 4, 15824−15828

http://pubs.acs.org/journal/acsodf

Photodetecting Heterostructures from Graphene and Encapsulated Colloidal Quantum Dot Films

Andrés Black,[†,‡] Fernando J. Urbanos,[†] Jonathan Roberts,[§] María Acebrón,[†] Ramón Bernardo-Gavito,[§] Beatriz H. Juárez,[†,∥,⊥] Benjamin J. Robinson,[§] Robert J. Young,[§] Amadeo L. Vázquez de Parga,[†,‡,⊥] and Daniel Granados*[,†]

[†]IMDEA Nanoscience, 28049 Madrid, Spain

[‡]Departamento de Física de la Materia Condensada, [∥]Departamento de Química-Física Aplicada, and [⊥]Condensed Matter Physics Center (IFIMAC), Universidad Autónoma de Madrid, 28049 Madrid, Spain

[§]Physics Department, Lancaster University, Lancaster LA1 4YB, U.K.

Supporting Information

ABSTRACT: Heterostructure devices consisting of graphene and colloidal quantum dots (QDs) have been remarkably successful as photodetectors and have opened the door to technological applications based on the combination of these low-dimensional materials. This work explores the photodetection properties of a heterostructure consisting of a graphene field effect transistor covered by a film of silica-encapsulated colloidal QDs. Defects at the surface of the silica shell trap optically excited charge carriers, which simultaneously enables photodetection via two mechanisms: photogating, resulting in a net p-doping of the device, and Coulombic scattering of charge carriers in the graphene, producing an overall decrease in the current magnitude.

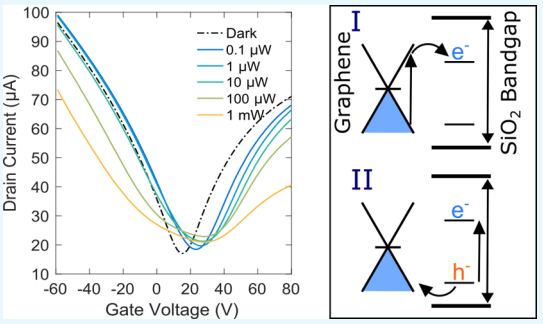

INTRODUCTION

State-of-the-art photodetectors today can be fabricated from bulk semiconductor materials and novel nanomaterials,[1−3] such as perovskites.[4] In addition, combinations of different types of low-dimensional nanomaterials have resulted in scientifically interesting and technologically exciting discoveries. One such hybrid system combines the superior electronic properties of graphene with a photosensitive material. For example, joining graphene and optically sensitive diamond nitrogen-vacancy centers resulted in photodetection via resonant energy transfer.[5] This mechanism was possible due to the close physical proximity between graphene and diamond, allowing for the nonradiative transfer of energy from the optically excited diamond to graphene. The resulting electron−hole pairs in the graphene device produced a measurable, albeit small photocurrent. Another popular hybrid system combines the unique, tunable optical properties of 0D colloidal quantum dots (QDs) with graphene into solar cells[6] and highly sensitive photodetectors.[7] Although resonant energy transfer is possible,[8] the most efficient photodetectors rely on the transfer of photoexcited charges between the optically active QDs and the high mobility graphene.[7] The high sensitivity and large photocurrents of such devices stems from a photogating mechanism, in which one type of photoexcited charge, for example, the hole, remains trapped in the QD layer while the other charge is transferred to the graphene and travels freely through the device.[9] The trapped charge electrostatically gates the underlying graphene device, effectively changing its doping. The high mobility in the graphene allows the transferred charge to travel many times through the device before recombining, resulting in a sensitivity-enhancing gain mechanism, with reported values as high as 10^8 charge carriers generated per incident photon.[10] Varying the spectral sensitivity of the QDs has produced photodetectors sensitive to a wide range of light.

This work explores the photodetecting properties of heterostructures, depicted in Figure 1a, consisting of a graphene field effect transistor (GFET) covered with a film of semiconducting, encapsulated colloidal QDs (ECQDs), which consist of alloyed QDs with a rich CdSe core and gradated ZnS shell, surrounded by silica. The silica encapsulation was performed through a reverse microemulsion process in the presence of the alloyed QDs,[11] and the finalized ECQDs were transferred onto chemical vapor deposition GFETs via a Langmuir−Blodgett process.[12] The 35 nm thick insulating silica shell of the ECQDs prevented photodetection through either charge transfer or resonant energy transfer between the graphene and semiconducting QD, which is simply used to increase the effective absorptive cross section of the silica spheres. Rather, light-sensitive defect states at the silica/graphene surface allowed for photodetection via two simultaneous mechanisms that tended to reduce the overall

Received: May 19, 2019
Accepted: July 26, 2019
Published: September 17, 2019

Downloaded via UNIV AUTONOMA DE MADRID on April 7, 2021 at 10:02:35 (UTC).
See https://pubs.acs.org/sharingguidelines for options on how to legitimately share published articles.

© 2019 American Chemical Society

DOI: 10.1021/acsomega.9b01449
ACS Omega 2019, 4, 15824−15828

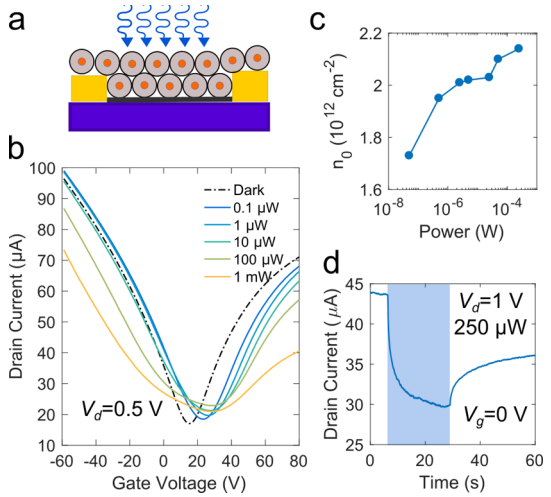

Figure 1. (a) Schematic of the device, showing the ECQD film covering a GFET. The ECQDs have a CdSZnSe semiconducting core (orange) surrounded by silica (gray). (b) Current versus gate voltage at various illumination powers. (c) Residual doping versus illumination power. (d) Temporal response to light, with blue shading corresponding to illumination. Excitation wavelength 488 nm.

current: electron trapping at the defects produces photogating, while also scattering charge carriers in the graphene channel. Through these two parallel, simultaneous mechanisms, the ECQD film makes the graphene photoconductive.

RESULTS AND DISCUSSION

Photodetection in the graphene/ECQD heterostructure is shown in Figure 1, with an optical image of the device shown in Figure S1. Illuminating the device causes the Dirac point voltage V_{DP}, defined as the gate voltage at which the conductivity is minimum, to shift to more positive values, as shown in Figure 1b. The conductivity minimum corresponds to the point at which the Fermi energy crosses graphene's Dirac point, where its density of states approaches zero. The residual doping concentration n_0 in the graphene can thus be calculated from the Dirac point voltage as $n_0 = C_{ox}V_{DP}/q$, where q is the elemental charge.[13] The gate oxide capacitance per unit area is given by $C_{ox} = \varepsilon_0\varepsilon_r/d$, where ε_r is the relative permittivity of the SiO_2 substrate, ε_0 is the free space permittivity, and d is the oxide thickness of 285 nm. The shift toward more positive V_{DP}, and thus increased n_0 as shown in Figure 1c, indicates that the graphene becomes increasingly p-doped with increasing illumination. The temporal response of the photodetection, shown in Figure 1d and for multiple cycles in Figure S2, is on the order of 15 s, with an even longer recovery time, on the order of several minutes. The current in Figure 1d, measured at a gate voltage $V_g = 0$ V, decreased upon illumination, which is consistent with the behavior shown in Figure 1a.

The increased p-doping and decreased current with illumination power and relatively slow photoresponse times indicate that photogating is at least partially responsible for the observed photodetection.[7,9] In this case, the p-doping implies that electrons are being trapped, allowing holes to circulate freely through the channel. Photogating can result in a sensitivity-enhancing gain mechanism if the time that the photoexcited charge carrier remains trapped before recombining τ_{rec} is larger than the transit time that it takes the opposite charge carrier to travel across the device τ_{trans}. This can produce fairly large photocurrents I_{pc}, proportional to the gain G

$$I_{pc} \approx G = \frac{\tau_{rec}}{\tau_{trans}} = \frac{\mu V_d}{L^2}\tau_{rec} \quad (1)$$

where μ is the charge carrier mobility and V_d is the applied drain voltage.[9] The transit time across $L = 40$ μm long device from Figure 1 is about $\tau_{trans} = L^2/\mu V_d = 21$ ns. This results in a gain of 10^9, considering a recombination time of about 20 s. The drawback of the photogating mechanism is that the response time is limited by the recombination of the photocarrier. Although this gain value is quite high in comparison to other CdSe QD[14] and QD/graphene[10] heterostructure devices, its photoresponse time is several orders of magnitude slower.

Figure 2a shows the same transfer curves as Figure 1a, but centered about V_{DP}, showing that the measured photocurrent is due not only to photogating but also to a distortion in the curve shape. Increasing the illumination causes the curves to "open up", reducing the transconductance ($g = dI_d/dV_g$) magnitude for both the electron ($n > 0$) and hole ($n < 0$) branches, as shown in Figure 2b. Here, n is the gate-dependent charge carrier density in the GFET $n = C_{ox}(V_g - V_{DP})/q$.[13] The photocurrent is shown in Figure 2c, and the maximum responsivities (defined as the magnitude of the photocurrent divided by the illumination power) of the electron and hole branches is shown in Figure 2d. For low illumination powers, the photogating induced p-doping and curve distortion mechanisms reinforce each other in the electron branch, resulting in large photocurrents and responsivities. In the hole branch, however, these two mechanisms tend to cancel each

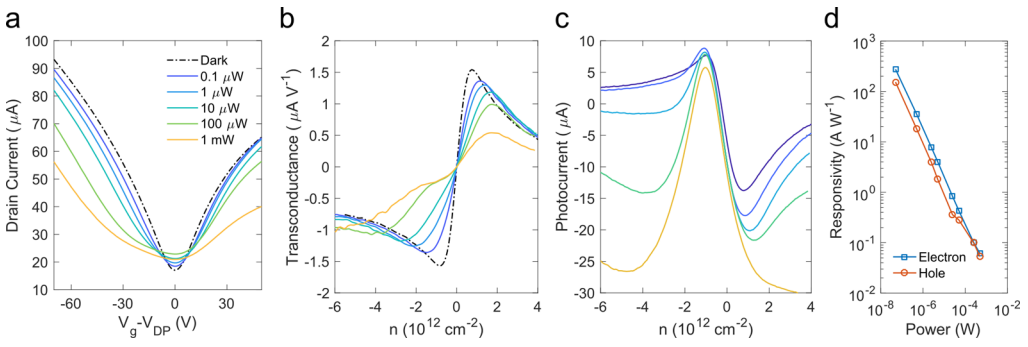

Figure 2. (a) Current vs gate voltage, centered at Dirac point. (b) Transconductance and (c) photocurrent vs charge carrier density. (d) Responsivity of electron and hole branches.

DOI: 10.1021/acsomega.9b01449
ACS Omega 2019, 4, 15824−15828

other out, with the photogating increasing the current and the curve distortion decreasing it.

The transconductance, shown in Figure 2b, is directly proportional to the charge carrier mobility, via the expression

$$\mu = \frac{q}{C_{ox}} \frac{L}{W} \frac{g}{V_d} \quad (2)$$

where L and W are the transistor length and width. The hole (electron) mobility of the GFET corresponds to the transconductance maximum (minima) in their respective branches. Thus, increasing the illumination clearly reduces the carrier mobility in both branches. Interestingly, at low illumination powers the shape of the transconductance and the photocurrent are similar. This is another indication that a photogating mechanism is present because the photocurrent will be directly proportional to the mobility and therefore to the transconductance, as seen from eqs 1 and 2.

Figure 3a illustrates two possible ways that photogating could occur, through photoexcitation of electron−hole pairs

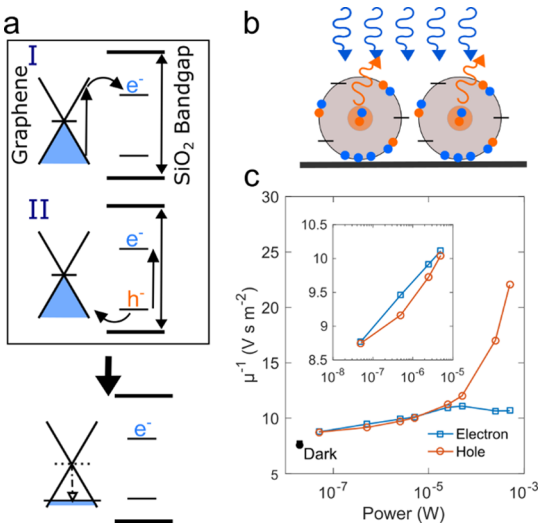

Figure 3. (a) Schematic of the photogating mechanism, with photoexcitation in (I) the graphene or (II) the ECQD silica shell surface. In both cases, the resulting trapped electron on the graphene/silica interface also acts as a charge scatterer. (b) Schematic showing the effect of illuminating the ECQDs. Electron (blue) and holes (orange) are created both on the semiconducting core, where they can combine either radiatively or non-radiatively, and on the silica surface. Horizontal black bars represent trap states that exist on the surface of the silica. In the vicinity of the silica/graphene surface, electrons accumulate leading to photogating and the scattering of charge carriers in the GFET. (c) Inverse mobility vs illumination power.

either in (I) the graphene or (II) at the surface of the ECQD silica shell.[15−19] In the former case, the electron may hop from the graphene to the ECQD silica shell, and in the latter, the hole may hop from the ECQD silica shell surface into the graphene device. The thick silica shell (about 35 nm) will prevent charge and energy transfer processes from occurring between the semiconducting core of the ECQDs and the graphene,[20,21] as confirmed via time-dependent measurements of the ECQD film photoluminescence (Figure S3). The semiconducting QD cores act here as antennas that increase the effective absorptive cross section of the silica spheres of the ECQDs, as observed in the absorption spectra in Figure S4, and thus the final photodetection of the device. Photoluminescence from the semiconducting core of the ECQDs may also be exciting electron−hole pairs at the silica surface or even generating charged species such as hydroxyl radicals.[22] This effect is expected to be minor compared to the external illumination, however, due to the low luminescent quantum yield of the ECQD film, as confirmed by the significant decrease in lifetime compared to the original ECQDs in solution,[11] a result of the film deposition process.[12] Besides, RET between the optically active defects on the silica shell surface and the graphene is only active for wavelengths below 380 nm (<3.26 eV),[17] whereas here the excitation wavelength is 488 nm (2.54 eV).

Any of the aforementioned scenarios end with immobilized charges on the silica shell. Although both electron and hole trapping may be present, electron trapping is dominant because a net p-doping is observed in the device. This is illustrated in Figure 3b, which shows the accumulation of electrons present on the silica surface (depicted in blue) near the graphene/ECQD interface. Increased illumination power produces more electron−hole pairs, more trapping, and thus increased photo-doping. The decrease in responsivity with increasing illumination power, shown in Figure 2d, indicates that an energy barrier must be overcome in order for charge transfer to occur between the graphene and silica shells.[7] The n-doping produced in the graphene FETs by depositing the ECQD films, as shown in Figure S5 and reported previously,[12] is the evidence that such a built-in energy barrier is present in the system. An exponential increase in the illumination power, and thus in the photoexcited charge carrier concentration, is required for the carriers to overcome the built-in energy barrier and produce a linear increase in the photocurrent.

Films of silica nanoparticles, carefully assembled through the Langmuir−Blodgett technique, have a collective effective refractive index, and can function as antireflective coatings in the visible light range.[23,24] This collective optical behavior can emerge when the wavelength of the light is much larger than the diameter of the individual nanoparticles. The changes in the refractive index, and thus the reflectivity, caused by the ECQD film are on the order of one. This effect is therefore not expected to significantly contribute to the photodetection, considering the exponential increase in light illumination required to appreciably increase the photocurrent. Therefore, photogating might be caused primarily by the accumulation of electrons at the ECQD/graphene interface.

The reduced mobility of both the electron and hole branches observed in Figure 2 indicates that charge carriers in graphene are being scattered upon illumination, with long-range Coulomb scattering from charged impurities being the dominant mechanism at room temperature.[25] The scattering could be due to light-induced point defect states, such as O and Si vacancies, at the surface of the silica shells.[15−19] Optical transitions can occur between silica point defects, whose localized states are in the bandgap, or between the defect states and the valence or conduction band of the silica. This can lead in some cases to the formation of self-trapped excitons.[15,16] Optically excited defect states in the silica bandgap could act as the trap sites for electrons in the photogating effect described above. These electrons, trapped on the silica surface at the graphene/silica interface, effectively act as charged p-doping impurities, scattering charge carriers in the graphene. The concentration of charged impurities causing scattering is predicted to be directly proportional to μ^{-1}. The inset of

DOI: 10.1021/acsomega.9b01449
ACS Omega 2019, 4, 15824−15828

Figure 3b shows that for low illumination power, μ^{-1} is linearly proportional to the logarithm of the illumination power, especially for electrons. This indicates that a logarithmic increase in the illumination causes a linear increase in charge scattering impurities at the silica surface. At higher illumination powers, the electron μ^{-1} saturates, possibly due to the saturation of electron trapping centers in the silica surface, which will tend to preferentially scatter electron charge carriers.[26] In contrast, the significant increase of μ^{-1} for holes indicates that some hole scattering impurity, originating at the ECQD silica shells surface, is still being efficiently created at high illumination powers.

This photoscattering mechanism is not observed in graphene photodetectors with colloidal materials such as PbS QDs. This is because the trapped electron resides at the semiconducting core of the QD (where the electron−hole pair is optically generated) and not at its surface.[7] The core is separated by several nanometers from the graphene by organic ligands, too far for the charge scattering effect to be efficient.[27] In the graphene/ECQD photodetectors, self-trapped excitons at the silica surface, consisting of a bound state of an electron and a hole, could also act as charge scattering centers for both types of graphene charge carriers. The gate bias could also have an effect on the scattering. Positive gate biases will tend to attract the negatively charged defect states in the silica closer to graphene, leading to increased electron charge scattering and lowering the electron mobility.[27] Photoscattering, like photogating, is caused by the accumulation of scattering centers at the ECQD/graphene interface.

The photodetector presented herein demonstrates yet another successful combination of 2D/0D hybrid heterostructures. In this device, photodetection through charge trapping at optically active defect states at the silica surface of the ECQDs. The trapped charges affect the conductivity of the GFET device not only through a photogating mechanism, but also through a photoscattering mechanism, that should be taken into account in engineering future photodetection devices based on graphene and colloidal QDs.

EXPERIMENTAL SECTION

ECQDs were synthesized via hot-injection method for the synthesis of the CQD core, followed by a microemulsion process to encapsulate the cores in a SiO_2 shell. Graphene was grown on copper foils in a chemical vapor deposition furnace, followed by a wet etch transfer process onto the substrate. GFET fabrication was carried out via photolithography, and the ECQD film was transferred onto the samples via the Langmuir−Blodgett method. Each of these steps is explained in detail in the Supporting Information.

ASSOCIATED CONTENT

Supporting Information

The Supporting Information is available free of charge on the ACS Publications website at DOI: 10.1021/acsomega.9b01449.

ECQD synthesis and LB deposition method; graphene device fabrication; transient photoluminescence; and transfer curve before and after ECQD deposition (PDF)

AUTHOR INFORMATION

Corresponding Author

*E-mail: daniel.granados@imdea.org.

ORCID

Andrés Black: 0000-0002-0726-5357
Beatriz H. Juárez: 0000-0003-1704-060X
Benjamin J. Robinson: 0000-0001-8676-6469
Robert J. Young: 0000-0002-5719-2205
Amadeo L. Vázquez de Parga: 0000-0003-0551-1603
Daniel Granados: 0000-0001-7708-9080

Notes

The authors declare no competing financial interest.

ACKNOWLEDGMENTS

R.J.Y. acknowledges support from the Royal Society through a University Research Fellowship (UF160721). This material was supported by the Air Force Office of Scientific Research under award no. FA9550-16-1-0276. This work was also supported by grants from The Engineering and Physical Sciences Research Council in the UK (EP/K50421X/1 and EP/1745 L01548X/1). B.J.R. acknowledged funding from Lancaster University and the Royal Society (RG160834). This work is partially supported by the Spanish Ministry of Economy, Industry and Competitiveness through Grant SUPERMNAN ESP2015-65597-C4-3-R, DETECTA ESP2017-86582-C4-3-R, MAT2017-85617-R and the Comunidad de Madrid through Grant P2018/NMT-4291 TEC2-SPACE-CM. D.G. acknowledges Grant RYC-2012-09864. IMDEA Nanociencia acknowledges support from the "Severo Ochoa" Programme for Centres of Excellence in R&D (MINECO, Grant SEV-2016-0686), and IFIMAC through the "Maria de Maetzu" Programme. This work was also partially supported by the Spanish Ministry of Economy, Industry and Competitiveness through Grant FIS2015-67367-C2-1-P, 09864. A.B. acknowledges Graphene Core H2020-FETFLAG-2014 and the Universidad Autonóma de Madrid FPI scholarship grant.

REFERENCES

(1) Yang, W.; Chen, J.; Zhang, Y.; Zhang, Y.; He, J.-H.; Fang, X. Silicon-Compatible Photodetectors: Trends to Monolithically Integrate Photosensors with Chip Technology. *Adv. Funct. Mater.* **2019**, *29*, 1808182.

(2) Yang, W.; Hu, K.; Teng, F.; Weng, J.; Zhang, Y.; Fang, X. High-Performance Silicon-Compatible Large-Area UV-to-Visible Broadband Photodetector Based on Integrated Lattice-Matched Type II Se/n-Si Heterojunctions. *Nano Lett.* **2018**, *18*, 4697−4703.

(3) Zhao, B.; Wang, F.; Chen, H.; Zheng, L.; Su, L.; Zhao, D.; Fang, X. An Ultrahigh Responsivity (9.7 mA W−1) Self-Powered Solar-Blind Photodetector Based on Individual ZnO-Ga2 O3 Heterostructures. *Adv. Funct. Mater.* **2017**, *27*, 1700264.

(4) Lin, C.-H.; Cheng, B.; Li, T.-Y.; Retamal, J. R. D.; Wei, T.-C.; Fu, H.-C.; Fang, X.; He, J.-H. Orthogonal Lithography for Halide Perovskite Optoelectronic Nanodevices. *ACS Nano* **2019**, *13*, 1168−1176.

(5) Brenneis, A.; Gaudreau, L.; Seifert, M.; Karl, H.; Brandt, M. S.; Huebl, H.; Garrido, J. A.; Koppens, F. H. L.; Holleitner, A. W. Ultrafast electronic readout of diamond nitrogen-vacancy centres coupled to graphene. *Nat. Nanotechnol.* **2014**, *10*, 135.

(6) Bi, Y.; Pradhan, S.; Akgul, M. Z.; Gupta, S.; Stavrinadis, A.; Wang, J.; Konstantatos, G. Colloidal Quantum Dot Tandem Solar Cells Using Chemical Vapor Deposited Graphene as an Atomically Thin Intermediate Recombination Layer. *ACS Energy Lett.* **2018**, *3*, 1753−1759.

(7) Konstantatos, G.; Badioli, M.; Gaudreau, L.; Osmond, J.; Bernechea, M.; de Arquer, F. P. G.; Gatti, F.; Koppens, F. H. L.

DOI: 10.1021/acsomega.9b01449
ACS Omega 2019, 4, 15824−15828

Hybrid graphene-quantum dot phototransistors with ultrahigh gain. *Nat. Nanotechnol.* **2012**, *7*, 363−368.
(8) Chen, Z.; Berciaud, S.; Nuckolls, C.; Heinz, T. F.; Brus, L. E. Energy Transfer from Individual Semiconductor Nanocrystals to Graphene. *ACS Nano* **2010**, *4*, 2964−2968.
(9) Buscema, M.; Island, J. O.; Groenendijk, D. J.; Blanter, S. I.; Steele, G. A.; van der Zant, H. S. J.; Castellanos-Gomez, A. Photocurrent generation with two-dimensional van der Waals semiconductors. *Chem. Soc. Rev.* **2015**, *44*, 3691−3718.
(10) Goossens, S.; Navickaite, G.; Monasterio, C.; Gupta, S.; Piqueras, J. J.; Pérez, R.; Burwell, G.; Nikitskiy, I.; Lasanta, T.; Galán, T.; Puma, E.; Centeno, A.; Pesquera, A.; Zurutuza, A.; Konstantatos, G.; Koppens, F. Broadband image sensor array based on graphene-CMOS integration. *Nat. Photonics* **2017**, *11*, 366.
(11) Acebrón, M.; Galisteo-López, J. F.; Granados, D.; López-Ogalla, J.; Gallego, J. M.; Otero, R.; López, C.; Juárez, B. H. Protective Ligand Shells for Luminescent SiO2-Coated Alloyed Semiconductor Nanocrystals. *ACS Appl. Mater. Interfaces* **2015**, *7*, 6935−6945.
(12) Black, A.; Roberts, J.; Acebrón, M.; Bernardo-Gavito, R.; Alsharif, G.; Urbanos, F. J.; Juárez, B. H.; Kolosov, O. V.; Robinson, B. J.; Miranda, R.; Vázquez de Parga, A. L.; Granados, D.; Young, R. J. Large-Area Heterostructures from Graphene and Encapsulated Colloidal Quantum Dots via the Langmuir-Blodgett Method. *ACS Appl. Mater. Interfaces* **2018**, *10*, 6805−6809.
(13) Hwang, E. H.; Adam, S.; Sarma, S. D. Carrier Transport in Two-Dimensional Graphene Layers. *Phys. Rev. Lett.* **2007**, *98*, 186806.
(14) Oertel, D. C.; Bawendi, M. G.; Arango, A. C.; Bulović, V. Photodetectors based on treated CdSe quantum-dot films. *Appl. Phys. Lett.* **2005**, *87*, 213505.
(15) Glinka, Y. D.; Lin, S.-H.; Chen, Y.-T. The photoluminescence from hydrogen-related species in composites of SiO2 nanoparticles. *Appl. Phys. Lett.* **1999**, *75*, 778−780.
(16) Glinka, Y. D.; Lin, S.-H.; Hwang, L.-P.; Chen, Y.-T.; Tolk, N. H. Size effect in self-trapped exciton photoluminescence from ${\mathrm{SiO}}_{2}$-based nanoscale materials. *Phys. Rev. B: Condens. Matter Mater. Phys.* **2001**, *64*, 085421.
(17) Kim, S.; Shin, D. H.; Kim, J.; Jang, C. W.; Kang, S. S.; Kim, J. M.; Kim, J. H.; Lee, D. H.; Kim, J. H.; Choi, S.-H.; Hwang, S. W. Energy transfer from an individual silica nanoparticle to graphene quantum dots and resulting enhancement of photodetector responsivity. *Sci. Rep.* **2016**, *6*, 27145.
(18) Rahman, I. A.; Padavettan, V. Synthesis of Silica Nanoparticles by Sol-Gel: Size-Dependent Properties, Surface Modification, and Applications in Silica-Polymer Nanocomposites—A Review. *J. Nanomater.* **2012**, *2012*, 1−15.
(19) Vaccaro, L.; Morana, A.; Radzig, V.; Cannas, M. Bright Visible Luminescence in Silica Nanoparticles. *J. Phys. Chem. C* **2011**, *115*, 19476−19481.
(20) Gaudreau, L.; Tielrooij, K. J.; Prawiroatmodjo, G. E. D. K.; Osmond, J.; de Abajo, F. J. G.; Koppens, F. H. L. Universal Distance-Scaling of Nonradiative Energy Transfer to Graphene. *Nano Lett.* **2013**, *13*, 2030−2035.
(21) Swathi, R. S.; Sebastian, K. L. Long range resonance energy transfer from a dye molecule to graphene has (distance)−4 dependence. *J. Chem. Phys.* **2009**, *130*, 086101.
(22) Narayanasamy, J.; Kubicki, J. D. Mechanism of Hydroxyl Radical Generation from a Silica Surface: Molecular Orbital Calculations. *J. Phys. Chem. B* **2005**, *109*, 21796−21807.
(23) Deák, A.; Bancsi, B.; Tóth, A. L.; Kovács, A. L.; Hórvölgyi, Z. Complex Langmuir-Blodgett films from silica nanoparticles: An optical spectroscopy study. *Colloids Surf., A* **2006**, *278*, 10−16.
(24) Boyd, R. W.; Gehr, R. J.; Fischer, G. L.; Sipe, J. E. Nonlinear optical properties of nanocomposite materials. *Pure Appl. Opt. J. Eur. Opt. Soc. A* **1996**, *5*, 505.
(25) Das Sarma, S.; Adam, S.; Hwang, E. H.; Rossi, E. Electronic transport in two-dimensional graphene. *Rev. Mod. Phys.* **2011**, *83*, 407−470.
(26) Farmer, D. B.; Golizadeh-Mojarad, R.; Perebeinos, V.; Lin, Y.-M.; Tulevski, G. S.; Tsang, J. C.; Avouris, P. Chemical Doping and Electron−Hole Conduction Asymmetry in Graphene Devices. *Nano Lett.* **2009**, *9*, 388−392.
(27) Hwang, E. H.; Adam, S.; Das Sarma, S. Transport in chemically doped graphene in the presence of adsorbed molecules. *Phys. Rev. B: Condens. Matter Mater. Phys.* **2007**, *76*, 195421.

DOI: 10.1021/acsomega.9b01449
ACS Omega 2019, 4, 15824−15828